Implications of isotope data on the metamorphism of the basic volcanites from the Sjangeli Window, northern Sweden

ROLF L. ROMER

Romer, R.L. 1989: Implications of isotope data on the metamorphism of the basic volcanites from the Sjangeli Window, northern Sweden. *Nor. geol. unders. Bull. 415,* 39-56.

The Lower Proterozoic supracrustal rocks of the Sjangeli area form an approximately N-S striking belt. The supracrustal belt consists of three metamorphosed volcanic and volcanosedimentary units, which are intercalated with metasedimentary units, and has been intruded by granites and syenites 1780 ± 85 My ago.

The basic volcanic rocks in the central section of the Sjangeli supracrustal belt have a Middle Proterozoic amphibolite facies mineral assemblage (c. 6 kbar and c. 560 °C), while the retrogressed basic volcanic rocks at the borders of the supracrustal belt (tuffs, lava flows, and pillow lavas) have Caledonian greenschist facies mineral assemblages (c. 4 kbar and c. 480 °C).

Rb-Sr whole-rock isotope data from the metamorphosed lava flows and from a basic dike yield ages of 2324 ± 15 My and 2252 ± 71 My, respectively. Mixing plots indicate, however, that these data could be too high by 100 to 150 My. Rb-Sr whole-rock isotope data from the tuffs define a mixing line with an apparent age of 488 ± 64 My. Mixing diagrams indicate c. 400 My as time of mixing. Lead isotope data from the lava flows and the basic dike give mixing time of 425-500 My. These mixing times are interpreted to be related with the Caledonian metamorphism.

Sm-Nd data from the amphibolites indicate a Middle Proterozoic age of the amphibolite facies metamorphism, which probably was related to the intrusion of the granites and syenites in the Sjangeli area. A Middle Proterozoic model age (1810 ± 20 My) is also obtained for the Pb-Pb data from the metalava flows.

R.L. Romer, Department of Economic geology, University of Technology Luleå, S-951 87 Luleå, Sweden.

Introductions

In the southwestward younging Baltic Shield of northern Scandinavia (Skiöld 1986, 1987, Gaal & Gorbatschev 1987), the Rombak-Sjangeli area forms part of an accretionary zone to the Archean craton. It is characterized by N-S striking volcano-sedimentary belts of probable island arc setting (Korneliussen et al. 1986), which have been intruded by Proterozoic acidic to basic rocks about 1700-1800 My ago. The volcanites vary from basic and ultrabasic composition at the eastern border to intermediate and acidic composition in the west (e.g. Korneliussen et al. 1986). The Sjangeli area includes the easternmost of these metamorphosed Lower Proterozoic volcanosedimentary belts which consists of basic volcanites (tuffs and lavas), carbonates, and pelitic sediments. The Sjangeli supracrustal belt strikes approximately N-S and the units dip steeply to the west (70-85°). It is about 10 km long and reaches a width of 5 km (Fig. 1). The Proterozoic rocks of the Rombak-Sjangeli area and their epiclastic cover (see below) are exposed in a tectonic window in the Caledonides (cf. Fig. 1).

A minimum age for the supracrustal rocks is given by the age of the granite, which yield Rb-Sr whole-rock ages of 1691 ± 90 My (Heier & Compston 1969) and 1780 ± 85 My (Gunner 1981). A least radiogenic lead composition from galena from Kopparåsen gives a model age of 2050 My (Romer 1989).

Following a phase of deep erosion, the Rombak-Sjangeli area became covered by epiclastic sediments (conglomerates, arkosic sandstones) during the Cambrian (Bergström & Gee 1985). The sediments subsequently became metamorphosed during the Caledonian orogeny and now form discontinuous, thin, flat-lying veneers of quartzites and metacon-

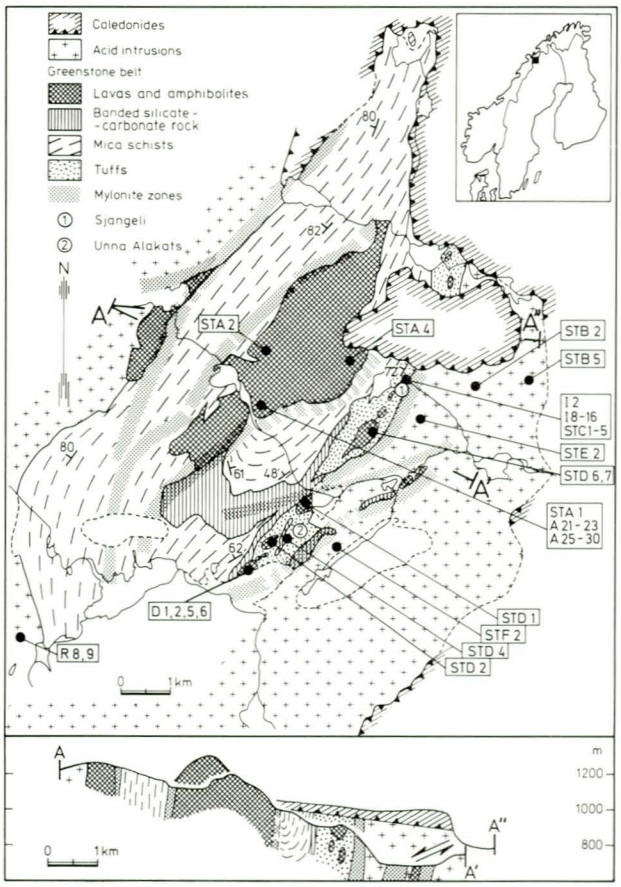

Fig. 1. Generalized geologic map of the Sjangeli area showing the major units and deformation zones. Note that the thin autochthonous basement cover below the Caledonian thrust plane is not shown. Simplified profiles A-A' and A-A'' with 3.5 fold vertical exageration.

glomerates on the Proterozoic basement (cf. Kulling 1964, Tull et al. 1985). Locally, the quartzites have been bent upright along steep listric faults, along which the basement had been reactivated (Bax 1986, 1989). The basement reactivation is related to the Caledonian overthrusting, which west of the Rombak-Sjangeli area startes about 450 My ago (e.g. Tull et al. 1985). The overriding of the Caledonian nappes over the basement resulted, in the eastern part of the eastern basement windows, only in a low-grade metamorphism reaching greenschist facies, while farther to the west amphibolite facies metamorphism occurred (e.g. Bryhni & Andreasson 1985, Tull et al. 1985, Lindqvist 1987). Such an increase of metamorphic grade to the west has also been observed for the Rombak-Sjangeli area (Sawyer 1987).

Earlier works in the Sjangeli area include a map in the scale of 1:200 000 by Petersson (1897) and reconnaissance Rb-Sr whole-rock isotope study by Gunner (1981). Other works by Geijer (1924) and Grip & Grietsch (1973) focussed on the Cu-mineralizations which occur in the basic tuffs (cf. also Romer 1987, 1989). Recent work in the Sjangeli area includes a map at the scale of 1:10 000 by Romer (1987) and a lead isotope study on the mineralizations of the Sjangeli area (Romer 1989).

Geology of the Sjangeli area

The metamorphosed Sjangeli supracrustal belt is characterized by a strike-parallel 'zebra-stripe' pattern consisting of volcanic units which are intercalated with sedimentary and volcano-sedimentary units.

To the east (Fig. 1), the metamorphosed volcanic rocks are lava flows intercalated with basic tuffs, which in many places are strongly mylonitized. The basic tuffs contain thin layers of banded carbonate-silicate rock. The basic tuffs are Mg-rich (7—22% MgO) and have high

contents of Cr (70—1100 ppm) and Ni (50—400 ppm). In a Jensen diagram (Jensen 1976) these rocks plot in the field for basaltic komatiites and high-magnesium tholeiitic basalts. The lava flows have lower contents of Mg (5-15 % MgO), Cr (‹ 300 ppm). and Ni (‹ 200 ppm) and plot in a Jensen (1976) diagram mainly in the field for high-iron and high-magnesium tholeiitic basalts. Both the basic tuffs and the lavas have high contents of K_2O and Na_2O, which may be due to sea-floor alteration.

The basic tuffs consist of actinolite, albite, epidote, chlorite, magnetite, titanite, quartz, and locally abundant biotite. The actinolites in places have cores of more hornblenditic composition. The pronounced schistosity in the tuffs has a regional 020° strike and dips 70° to the west. However, near the lava flows, the schistosity parallels the contact between the lava flows and the enclosing tuffs, similar to the plastically deformed ductile material in the necks between boudins, and deviates from the general trend. The lavas have the same mineral assemblages as the tuffs, though they have lower contents of magnetite and biotite. They show little mineral orientation and have no schistosity, except for flow STD2 which also has higher contents of biotite. The weak mineral orientation decreases from the border to the center of the lava flows.

The amphibolite-facies rocks in the central part of the Sjangeli supracrustal belt (Fig. 2: cross-hatched) comprise amphibolites, which contain lenses of serpentinites, minor pillow lavas and thin layers of banded carbonate-silicate rock. The amphibolites have high contents of Mg (9—19 % MgO), Cr (200—1700 ppm) and Ni (70—500 ppm) (Romer 1987) and show platinum group element ratios similar to those of komatiites (Barnes et al. 1988). Although they are chemically very similar to the basic tuffs, they have lower K_2O and variable Na_2O contents.

The amphibolites consist predominantly of hornblende and andesine. Ilmenite and magnetite are the other main constituents, while quartz is minor and epidote occurs locally.

The volcanic rocks at the western border of the Sjangeli supracrustal belt (Fig. 2: diagonal-hatched) include pillow lavas which locally are interlayers with thin discontinuous layers of banded carbonate-silicate rock. The pillows have a monomineralic amphibole rim and a 'core' of albite, actinolite, and minor quartz. The matrix between the pillows consists mainly of chlorite, epidote, and calcite. There is a mineral orientation in the pillows which results in a weak schistosity (strike 020°, dip 80° W).

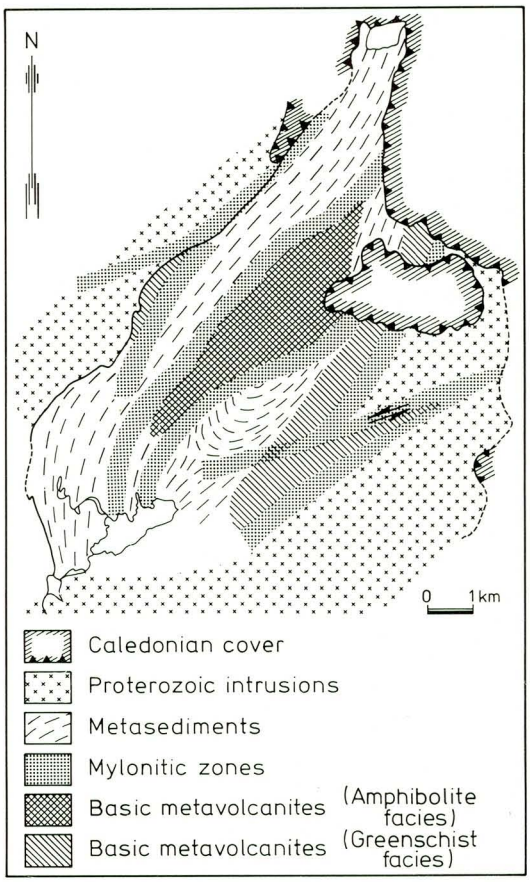

Fig. 2. Schematic map of the Sjangeli area showing the distribution of the mylonites and the metamorphic facies of the basic volcanic units (for mineral assemblages see text). The mylonites have a greenschist-facies mineral assemblage.

The mineral assemblage of the amphibolites (Fig. 2: cross-hatched) coincides with the 'common' amphibolite-facies mineral assemblage of basic rocks from Laird & Albee (1981) and Moody et al. (1983), and consists of hornblende, andesine, ilmenite, magnetite, epidote, quartz and locally minor biotite. The mineral assemblages of the other two volcanic units (Fig. 2: diagonal-hatched) consist of actinolite, albite, epidote, chlorite, titanite, quartz, magnetite, minor calcite, and variable amounts of biotite, which correspond to the 'common assemblage' (Laird & Albee 1981, Moody et al. 1983) for greenschist facies rocks of basic composition.

Quartz-mica schists and banded carbonate-silicate rocks are intercalated with the volcanic and volcano-sedimentary units. Although these rocks represent better indicators of metamorphism than the basic rocks, they have not been studied closer, since this study mainly concentrates on the contrasting behavior of isotopic systems in variably metamorphosed rocks. Generally, the schistosity and the banding of quartz-mica schists and banded carbonate-silicate rocks are parallel to the unit contacts; however, in the southern part of the Sjangeli area, the carbonate-silicate rocks are tectonically thickened and show extensive internal deformation (cf. Romer 1987).

To the northwest and east the Sjangeli supracrustal belt is bordered by mylonitic zones (Figs. 1 & 2), which form the contact between the granites and the mica schists and basic tuffs, respectively. To the southwest, the supracrustal belt is intruded by midproterozoic granites and syenites (cf. Gunner 1981).

In addition to the mylonites, which border parts of the supracrustal belt, there are mylonites which approximately follow the contact between the amphibolites and the quartz-mica schists. One late mylonite zone cuts the N-S trending mylonite zones which form the eastern border of the Sjangeli supracrustal belt. This zone has an apparent sinistral offset of 2.5 km (Fig. 2: arrows).

Mineral assemblages and mineral chemistry

The amphibolite-facies mineral assemblage of the central volcanic unit (Fig. 2: cross-hatched) consists predominantly of hornblende and andesine. Ilmenite and magnetite are the opaque minerals. Epidote is locally present, quartz is minor, and biotite is scarce or absent.

Towards the mylonites, actinolite, chlorite, calcite and titanite appear. Actinolite commonly overgrows hornblende and forms small needles, which give the crystal 'tips' of the hornblendes a brushy appearance. The hornblende is also partially cataclastic and the cracks are sealed with fibrous calcite, and partially with chlorite or fibrous actinolite. Feldspar is saussuritized. This mineral assemblage, which only occurs as overgrowth near mylonitic zones, indicates that the mylonitization occurred after the metamorphic peak under greenschist-facies conditions.

The mylonitized tuffs and the massive lava flows show the greenschist-facies 'common assemblage' of Moody et al. (1983) consisting of actinolite - albite - epidote - chlorite - titanite - quartz - (biotite). Epidote forms snowball-like overgrowths in the albite - actinolite-chlorite-quartz-(biotite) matrix of the tuffs. Epidote locally occurs together with chlorite and magnetite; furthermore, epidote is abundant in veins.

Mineralogical variability. The plagioclase has a bimodal compositional variation. The plagioclases from the amphibolites (Fig. 2) have An-contents which vary from An34 to An38. In contrast, the plagioclases from the lava flows and tuffs have An-contents below An05. Plagioclase with such low An-contents have also been found in the retrogressed border zones of the amphibolites.

The pistacite contents of the epidotes in the lava flows and the tuffs also have a bimodal distribution. High pistacite contents ($X_{Pistacite}$ = 0.25—0.33) have been observed from epidotes which are associated with chlorite and magnetite, overgrow the plagioclase - amphibole-biotite groundmass, or occur in early veins, together with quartz. Together with magnetite a $X_{Pistacite}$ = 0.33 indicates a fO_2 near the hematite-magnetite buffer (Bird & Helgeson 1981). These epidote veins are cut by later veins which contain clinozoisite with calcite and quartz, indicating a lower fO_2. The epidotes from the tuffs differ in their pistacite content from the epidotes from the pillow lavas which have $X_{Pistacite}$ varying from 0.12 to 0.17. If the epidotes had been in equilibrium with quartz, calcite, and a fluid, then the XCO_2 of the fluid would have been confined to XCO_2 ‹0.05 for epidotes with $X_{Pistacite} \approx 0.33$ or $X_{Pistacite} \approx 0.12 - 0.17$. However, for epidotes with $X_{Pistacite} \approx 0.25$ the XCO_2 of the fluid is hardly constrained, and can vary up to $XCO_2 \approx 0.7$ (Bird & Helgeson 1981).

The calcic amphiboles, which represent the mineral group in rocks from the Sjangeli area with the largest chemical variation (cf. Fig. 3 and Table 1), are tschermatitic hornblendes, magnesio-hornblendes, and actinolites in the nomenclature of Leake (1978). Cummingtonite has not been observed. A calculation of the amphibole composition into the end members tremolite, edenite, tschermakite, glaucophane, and cummingtonite (cf. Laird & Albee 1981) shows that the glaucophane component is always very low, and that the cummingtonite component is less than 0.1 (for all iron as

Table 1. Representative composition of silicates for the mineral assemblage of the amphibolites (STA*x-y*), the lava flows (STA*x-y*, core: STD4-2), and the tuffs (STC*x-y*). Analyses performed at SGU, Uppsala, on a ARL wavelength dispersive microprobe at 15kV aceleration voltage and 8nA sample current on brass (for complete listing of analyses and analytical precedure see Romer, 1987). Site distribution of amphiboles based on 23 oxygen according to Laird & Albee (1981), biotites (22 oxygen) and chlorites (28 oxygen) after Spear (1982). All Fe assumed as Fe^{2+}.

	amphiboles					biotites		chlorites		
Oxide	STA1-13	STA2-1	STD4-2	STD6-3	STC5-6	STD4-5	STC1-12	STD3-2	STD4-8	STC5-4
SiO_2	43.67	47.26	44.52	52.81	54.34	36.88	37.43	27.79	26.70	26.83
TiO_2	.59	.48	.48	.22	.00	.92	1.15	.11	.00	.07
Al_2O_3	11.64	9.24	10.61	3.26	.76	16.31	15.75	21.00	19.94	18.26
FeO	16.49	16.31	14.48	11.04	11.08	14.26	15.94	20.64	16.01	18.74
MnO	.30	.31	.17	.29	.39	.13	.25	.20	.11	.40
MgO	10.40	11.36	12.41	16.66	16.84	15.05	13.58	19.17	23.34	19.84
CaO	11.66	11.79	12.16	12.54	13.05	.01	.07	.18	.00	.08
Na_2O	1.39	1.21	1.61	.50	.10	.97	.06	.00	.00	.02
K_2O	.29	.14	.44	.11	.01	9.65	9.72	.07	.00	.02
Total	96.43	98.10	96.88	97.43	96.57	93.28	93.96	89.16	86.10	84.26
Si	6.591	6.954	6.642	7.589	7.869	5.506	5.425	5.230	5.118	5.361
Al (IV)	1.409	1.046	1.358	0.411	0.131	2.494	2.575			
								Al 5.867	5.674	5.417
Al (VI)	0.662	0.556	0.509	0.142	0.000	1.121	0.814			
Ti	0.067	0.053	0.054	0.024	0.000	0.103	0.125	0.016	0.000	0.011
Mg	2.340	2.492	2.760	3.571	3.637	3.385	2.934	5.377	6.668	5.910
Fe	2.082	2.008	1.807	1.327	1.342	1.063	1.933	3.255	2.566	3.131
Mn	0.039	0.038	0.022	0.036	0.047	0.016	0.031	0.032	0.018	0.067
					Σ(VI)	5.688	5.837			
Ca	1.885	1.859	1.944	1.930	2.024	0.002	0.011	0.036	0.000	0.017
Na	0.406	0.346	0.465	0.139	0.028	0.021	0.017	0.000	0.000	0.007
K	0.057	0.027	0.083	0.020	0.001	1.838	1.798	0.017	0.000	0.005
					ΣA	1.861	1.826	Σ 19.830	20.044	19.826

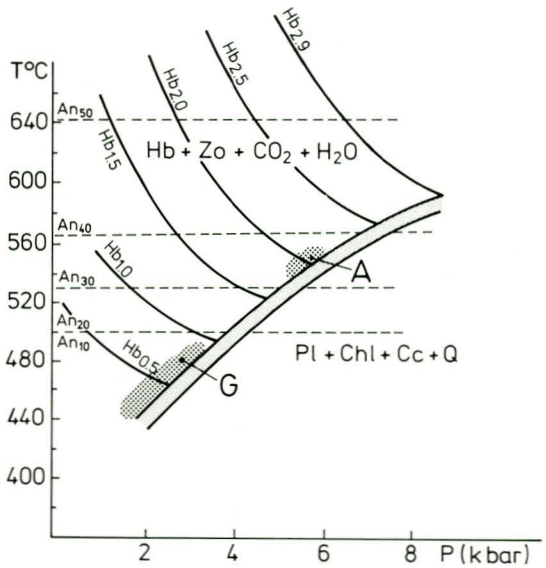

Fig. 3. Compositional variation of plagioclase and hornblende with P and T for the system CaO - MgO - Al_2O_3 - (Fe_2O_3) - SiO_2 - CO_2 - H_2O (after Plyusnina 1982). Shaded areas represent the composition of the co-existing plagioclases and hornblendes from the amphibolites (A) and from the lava flows and tuffs (G). For discussion and limitations see text. Hb_x refers to the Al_{total} content in the amphibole (normalized to 23 oxygen per formula unit).

FeO). The content of the actinolite component correlates negatively with both the edenite and the tschermakite component. The amphiboles from the amphibolites have an actinolite component which is less than 0.2, while the actinolite component in the amphiboles of the lava flows and tuffs varies from 0.05 to 0.95. The variation of the actinolite component is continuous.

Robinson et al. (1982) calculated the distribution coefficients (K_D) for Mg, Fe, Al, Na, and Ca between amphiboles and chlorite (Fe^{2+} ⟷ Mg, Al_2 ⟷ MgSi) and plagioclase (NaSi ⟷ CaAl). The K_D values vary systematically with the metamorphic grade, but they are not calibrated in terms of P and T. The calculated values for the amphibolites from the Sjangeli area for the plagioclase amphibole pair are $K_D \approx 0.032 - 0.053$, which is similar to K_D values from the garnet-oligoclase zone of basic schists from Vermont (Robinson et al. 1982, Laird & Albee 1981). The K_D ratios of the lava flows and the tuffs for the same mineral pair are less than 0.002, which corresponds to the biotite-albite and the garnet-albite zone of medium-P series basic schists

from Vermont (Robinson et al. 1982, Laird & Albee 1981). The chlorite amphibole K_D ratios for the Fe^{2+} ‹--› Mg, Al_2 ‹--› MgSi exchange vary from ~ 1.0 to ~ 1.5 and from ~ 1.0 to ~ 2.0, respectively.

Conditions of metamorphism. The reaction hornblende + epidote + CO_2 + H_2O = plagioclase + chlorite + calcite + quartz for mafic rocks has been calibrated by Plyusnina (1982). The corresponding amphibole and plagioclase compositions of amphibolites, lava flows and tuffs yield c. 560°C and c. 6 kbar for the amphibolites, and indicate a temperature of c. 480 °C and a pressure of c. 4 kbar for the greenschist-facies mineral assemblage of the tuffs and lava flows (Fig. 3). Since the amphibolites do not contain chlorites, which are in equilibrium with the plagioclase and hornblende, the above reaction becomes divariant and the pressure estimate represents a maximum value. Note that these P-T estimates are based on an iron-free system which was buffered at a X_{CO_2} = 0.1. The effect of Fe^{2+} ‹--› Mg substitution in the system on the Al_2O_3 (total) content of the amphiboles is minimal (Plyusnina 1982: 10—15°C lower temperatures), especially in comparison to the effect due to the deviation of the X_{CO_2} values. The X_{CO_2} values inferred from the pistacite contents of epidote indicate that the X_{CO_2} of the amphibolites were lower than the ones of the used geothermo/barometer (Plyusnina 1982), while the X_{CO_2} of the greenschist-facies rocks was not confined. This deviation may shift the equilibrium temperatures by probably some 50°C. However, the above P-T estimates are comparable with other P-T estimates (Moody et al. 1983) for the transition of greenschist to amphibolite facies.

P-T estimates from the west of the Sjangeli area give higher values. For example, Sawyer (1986) reported P and T values of ›6 kbar and 575—600°C from the southwestern and western part of the Rombak window. Higher P- and T-conditions, to the west of the Sjangeli area, corroborate the general pattern for the crystalline basement of the Caledonides of Scandinavia, which shows higher grade metamorphism to the west (cf. Bryhni & Andreasson 1985).

In the basic tuffs and the lava flows, the high-Al amphiboles are not in equilibrium with the albite (‹An05) and no relics of more calcic plagioclase have been found. The high-Al amphiboles are remnants from an amphibolite-facies metamorphism. The greenschist-facies mineral assemblage of the tuffs and the lava flows are the product of a pervasive retrogression.

Since the retrogression implies rehydration of low-H_2O or anyhydrous phases, the retrogressed rocks must have been permeable. Further, the permeability must have been evenly distributed, otherwise low-permeability regions would have been excluded from retrogression (e.g. Beach 1976, Hickman & Glassley 1984). On a large scale, the amphibolites represent a low permeability unit, while the tuffs represent a high permeability zone. On a smaller scale, the lava flows were less permeable than the basic tuffs. This is indicated by the partially reset Rb-Sr whole-rock isotope systems of the basic tuffs (p. 48).

Isotope methods and results

Pb was separated by ion exchange as described by Grünenfelder et al. (1986). Contents of Pb, U and Th were determined by isotope dilution using a composite ^{208}Pb-^{235}U-^{230}Th tracer. Pb was measured, using a Re single filament silica-gel technique (e.g. Cameron et al. 1969), on a Finnigan MAT 261 multi-collector mass spectrometer. Mass fractionation correction factors for Pb were calculated for the NBS Pb 981 standard, taking $^{208}Pb/^{206}Pb$ = 2.16715 (Todt et al. 1984). The lead composition was measured with a 2σ precision better than 0.08 % ($^{206}Pb/^{204}Pb$). U and Th were measured on an AVCO single collector solid source mass spectrometer, using a Re single filament 'carbon sandwich' technique (HNO_3-load of U and Th between two carbon layers; G.R. Tilton, pers. comm.). Uncertainties in the concentration data are ca. 0.3% for Pb and 1% for U and Th.

The Sr extraction ion exchange procedure has been described by Grünenfelder et al. (1986). Contents of Sr and Rb have been determined by isotope dilution using a composed ^{84}Sr-^{87}Rb tracer. Sr was analyzed on a Finnigan MAT 261. The Sr isotope fractionation was corrected by normalizing to $^{86}Sr/^{88}Sr$ = .1194. The $^{87}Sr/^{86}Sr$ ratio of the Sr standard NBS 987 was 0.71028.

Rb was analyzed on an AVCO single collector solid source mass spectrometer. Uncertainties in the concentration data are about 0.5 % for Sr and 1.0 % for Rb.

Sm and Nd were separated on a teflon powder column (Richard et al. 1976, White & Patchett 1984) after precleaning on the Sr ion exchange column. Sm and Nd were measured as Sm^+ and Nd^+ on a Finnigan Mat 261 mass spectrometer, and the contents were determined by isotope dilution with a ^{149}Sm-^{150}Nd tracer. Nd isotope ratios were normalized to $^{146}Nd/^{144}Nd$ = .72190. The $^{143}Nd/^{144}Nd$ ratio of the La Jolla Nd standard was 0.511863 ± 0.000025. (Vaccum problems resulted in large analytical uncertainties for the Nd runs). Uncertainties in the concentration data are about 0.15 % for Nd and 0.15 % for Sm. Decay constants used are the ones recommended by Steiger & Jäger (1977), and $\lambda\ ^{147}Sm = 6.54 \cdot 10^{-12}\ y^{-1}$ (e.g. Wasserburg et al. 1981), respectively.

All isotopic data discussed in the following sections are given in Tables 2, 3 & 4. They were acquired at the University of California, Santa Barbara. The sample locations are indicated in Fig. 1.

Table 2: Rb-Sr isotope data from lava flows, metamorphosed basic dikes, and tuffs (cf. Fig. 1).

Lava flows. sample		$^{87}Sr/^{86}Sr$	1σ	$^{87}Rb/^{86}Sr$	Sr	Rb
STD1	WR	.73654	.00015	.863	247.6	72.0
STD2	WR	.73773	.000032	.232	116.2	9.08
	fsp (4)	.741790	.000055	.118	213.5	8.44
	fsp (101)	.734787	.000033	.164	125.7	6.95
	fsp (107)	.73796	.00047	.178	161.1	9.66
STD4	WR	.77889	.000055	2.25	102.0	77.1
	fsp (5)	.76160	.00094	.324	42.70	4.64
	fsp (15)	.777036	.000071	1.20	20.84	8.38
	epi (3)	.75572	.000061	.0032	2033.	2.18
	epi (5)	.751503	.000084	.0053	2218.	3.96
	bio (102)	1.32728	.000022	74.3	4.23	100.
	bio (102*)	1.0685	.00011	55.0	4.245	76.2
	bio (103)	.96421	.000097	20.5	22.2	150.
	amf (6)	.77667	.00082	2.19	14.22	10.5
STD6	WR	.71608	.000019	.377	157.6	20.0
STD7	WR	.72492	.00031	.635	237.6	50.9
	fsp (8)	.720382	.000084	.665	329.2	73.9
	fsp (9)	.714975	.000031	.0739	258.0	6.44
	fsp (102)	.71761	.00013	.152	236.4	12.1
	fsp (106)	.72243	.00051	.629	312.0	66.2

Metamorphosed basic dike sample		$^{87}Sr/^{86}Sr$	1σ	$^{87}Rb/^{86}Sr$	Sr	Rb
D1	WR	.71703	.00018	.106	206.8	7.56
D2	WR	.724179	.000058	.355	591.5	72.5
D5	WR	.77665	.00021	1.90	118.1	77.2
D6	WR	.74534	.00089	.676	263.9	61.4

Tuffs sample		$^{87}Sr/^{86}Sr$	1σ	$^{87}Rb/^{86}Sr$	Sr	Rb
I2	WR	.72921	.00018	.363	266.3	32.5
I8	WR	.739144	.000028	1.56	91.18	47.8
I9	WR	.728362	.000038	1.05	132.6	46.9
I10	WR	.72857	.00026	.598	21.83	4.40
I11	WR	.72955	.00012	1.08	224.1	81.2
I12	WR	.73774	.00015	1.22	168.7	69.1
I13	WR	.729394	.000062	4.79	7.71	12.4
I14	WR	.718636	.000094	.226	180.2	13.8
I15	WR	.71626	.00037	.267	111.2	10.0
I16	WR	.73303	.00012	.538	42.15	7.64
STC1	WR	.73834	.000062	3.32	133.0	149.
	fsp (17)	.739293	.000057	.787	15.68	4.15
	bio (101)	1.2480	.0011	22.6	7.505	54.4
	bio (106B)	1.08666	.00016	48.8	22.7	345.
STC2	WR	.72967	.000039	1.19	211.8	85.0
STC3	WR	.71983	.00087	.551	380.2	70.6
STC4	WR	.745398	.000071	3.84	63.0	81.4
	fsp (14)	.735200	.000034	.546	69.85	12.8
STC5	WR	.72505	.00015	1.04	146.4	51.1

Table 3. Sm-Nd isotope data from amphibolite STA1 and from lava flow STD4. Sample locations are indicated in Fig. 1.

Amphibolite sample		$^{143}Nd/^{144}Nd$	1σ	$^{147}Sm/^{144}Nd$	Nd	Sm
STA1	WR	.512709	.000091	.1803	8.077	2.384
	amf (5S)	.513447	.000031	.2318	6.838	2.596
	amf (7S)	.513617	.000020	.2786	5.866	2.676
	bio (105)	.511430	.000025	.1009	451.7	74.61
	fsp (1)	.511041	.000014	.0692	5.617	.637
	fsp (16)	.511341	.000053	.0704	6.122	.706
	fsp (3)	.511365	.000026	.0682	6.178	.690

Lava flow sample		$^{143}Nd/^{144}Nd$	1σ	$^{147}Sm/^{144}Nd$	Nd	Sm
STD4	WR	.512488	.000052	.2002	6.04	1.98
	amf (10)	.512760	.000057	.2413	6.018	2.378
	amf (6)	.513423	.000090	.2348	7.633	2.935
	bio (102)	.512739	.000005	.2010	.543	.179
	bio (103)	.513106	.000056	.2245	3.932	1.446
	epi (3)	.512811	.000013	.1844	48.87	14.76
	epi (6)	.512411	.000015	.1818	28.53	8.496
	fsp (5)	.512721	.000019	.1846	11.04	3.338

Table 4. Pb-isotope data from the amphibolites, lava flows, metamorphosed basic dike, and tuffs. Sample locations are indicated in Fig. 1.

Lava flows

sample		$^{204}Pb/^{204}Pb$	$^{207}Pb/^{204}Pb$	$^{208}Pb/^{204}Pb$	Pb	U	Th
STD1	WR	22.629	16.096	43.472	3.27	.54	2.58
STD2	WR	45.350	18.430	51.479	3.91	4.52	5.94
	fsp (4)	36.425	17.684	47.810	2.29	1.36	1.19
	fsp (101)	31.689	17.168	44.968	1.70	.802	5.52
	fsp (107)	29.327	16.964	43.809	2.21	.781	1.21
STD4	WR	26.496	16.595	43.955	2.37	.36	.29
	epi (3)	24.345	16.353	42.820	28.3	2.62	1.56
	epi (6)	23.298	16.281	41.937	28.3	1.99	1.32
	fsp (5)	32.091	17.014	39.016	9.93	6.12	1.41
	fsp (15)	26.746	16.616	42.358	.345	.118	.0223
STD6	WR	24.297	16.216	42.244	3.71	1.33	3.97
STD7	WR	24.885	16.331	45.075	1.90	.448	2.29
	fsp (8)	20.187	15.834	40.925	1.44	.134	.671
	fsp (9)	22.058	15.992	39.323	.932	4.2	34.0
	fsp (106)	68.894	21.399	103.340	3.81	3.31	2.24
	pyr	23.810	16.335	47.858	5.5	.031	.288
	pyr (3)	20.062	15.785	39.710	17.6	1.88	2.23

Profile across flow/dike

sample	$^{204}Pb/^{204}Pb$	$^{207}Pb/^{204}Pb$	$^{208}Pb/^{204}Pb$	Pb	U	Th
D1	32.459	17.754	62.375	9.56	1.43	.715
D2	33.017	17.808	56.694	6.67	3.77	12.2
D5	40.649	18.659	110.49	9.32	7.06	122.
D6	82.802	24.210	119.63	6.15	5.77	12.8

Tuffs

sample	$^{204}Pb/^{204}Pb$	$^{207}Pb/^{204}Pb$	$^{208}Pb/^{204}Pb$	Pb	U	Th
I2	25.374	16.371	41.308	3.33	.761	1.22
I8	34.199	17.387	52.083	2.67	1.39	6.56
I9	38.866	17.672	56.439	1.76	1.35	12.7
I10	50.295	18.855	44.906	.766	1.66	.577
I11	34.112	17.361	44.568	1.80	1.10	1.86
I12	31.716	17.197	44.184	3.33	1.66	2.47
I13	25.222	16.359	43.776	1.67	.388	1.85
I14	24.756	16.239	39.285	2.76	1.26	.467
I15	19.910	15.667	38.451	2.44	.446	2.24
I16	25.345	16.305	39.840	1.07	.460	1.16
STC1	23.812	16.251	40.693	2.20	.440	1.01
STC2	30.817	17.070	45.937	2.15	.820	2.23
STC3	28.245	16.768	41.611	2.90	1.83	.276
STC4	34.853	17.452	45.806	1.13	.571	1.44
STC5	37.715	17.825	48.380	1.55	.987	2.20

Amphibolites

sample	$^{204}Pb/^{204}Pb$	$^{207}Pb/^{204}Pb$	$^{208}Pb/^{204}Pb$	Pb	U	Th
A21	18.802	15.600	37.188	5.54	.691	.369
A22	18.800	15.603	37.507	3.91	1.09	.372
A23	18.557	15.599	37.767	3.92	.215	.32
A25	17.014	15.411	36.200	9.12	.703	.478
A26	17.439	15.452	36.290	4.67	.701	.485
A27	17.099	15.484	36.308	2.2	.226	.303
A28	16.914	15.433	36.153	6.15	(8.32)	1.68
A29	19.346	15.621	37.332	4.4	2.40	.416
A30	15.618	15.173	35.050	34.6	2.84	4.33
STA1	17.032	15.450	36.600	3.86	.337	.400
STA2	15.643	15.333	35.270	54.2	.155	.315
STA4	17.810	15.600	37.025	2.2	1.03	.315

Acidic rocks

sample	$^{204}Pb/^{204}Pb$	$^{207}Pb/^{204}Pb$	$^{208}Pb/^{204}Pb$	Pb	U	Th
I1	20.312	15.808	40.231	5.22	.964	6.91
R8	19.435	15.571	39.604	7.48	1.95	12.51
R9	20.481	15.678	39.669	5.53	18.6	8.02
STB2	20.036	15.683	39.447	21.0	2.95	14.2
STB5	19.467	15.658	39.830	19.6	4.24	35.6
STE2	16.799	15.332	37.849	24.9	.964	6.91
STF2	25.558	16.505	48.069	67.7	5.85	13.5

Mixing lines

Vollmer (1976) and Faure (1986) have shown that the mixing of two isotopically different Sr components yields a straight line in a $^{87}Sr/^{86}Sr$ - 1/Sr diagram, on the following conditions: that the concentration and isotopic composition of the primary component in all samples is the same. The second, isotopically homogeneous component is added in different amounts to the various samples. The straight line relationship holds for the time of mixing alone, since later addition of ^{87}Sr, which results from decay of ^{87}Rb, scatters the samples around the mixing line in the mixing diagram. The addition of radiogenic Sr can change the Sr composition drastically without affecting the Sr concentration to a significant extent (cf. part B in Figs. 4 & 5). Therefore, to test a set of samples for mixing, the isotopic composition of the samples has to be recalculated for the time of mixing.

Assuming that there had been mixing and a linear array existed after the mixing, the recalculation of the Sr composition to the time of mixing would improve the fit of the mixing line in the $^{87}Sr/^{86}Sr$ - 1/Sr diagram, since the effect of the radiogenic Sr addition is eliminated. Note that the mixing event has to be the last isotopic disturbance of the system, i.e. Rb and Sr were immobile after the mixing event. For a stepwise recalculation of the samples, the fit of the mixing line would improve, as long as the time of mixing is approached, and the fit of the mixing line would decrease, as the time of mixing is passed (cf. part C in Figs. 4 & 5). As a measure for the fit of the mixing line, the regression coefficient could be used. A clear maximum of the regression coefficient at a time different from the age indicated by the 'isochron' indicates that the latter is a mixing line and had an initial slope, i.e. had an 'inherited age'.

The time of mixing coincides with the time at which the regression in the $^{87}Sr/^{86}Sr$ - 1/Sr diagram is maximal. Note that the fit to a straight line in the $^{87}Sr/^{86}Sr$ - $^{87}Rb/^{86}Sr$ isochron diagram does not have to be maximal at that time, since Sr and Rb do not have to behave coherent during the mixing.

The Pb-Pb system can also be tested for mixing. If there had been mixing of two isotopically different lead components, and this had resulted in an anomalous lead line, the in-situ radiogenic lead growth after the time of mixing would result in a scatter of the lead isotope composition around the lead line. The recalculation of the isotopic composition of the samples for the time of mixing should diminish the scatter and result in a better fit of the mixing line to the sample compositions. The recalculation time for which a minimum scatter is obtained represents the time of mixing. Such an interpretation model has also been used by Welke & Nicolaysen (1981).

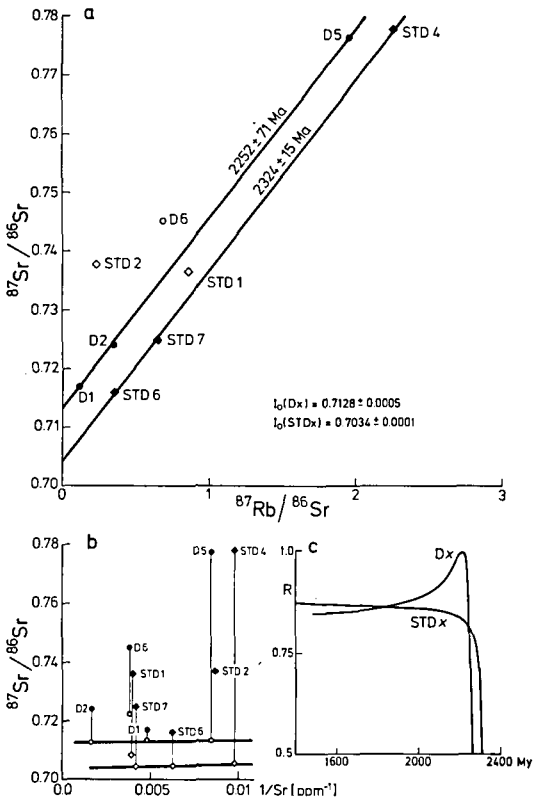

Fig. 4. A. $^{87}Sr/^{86}Sr$ - $^{87}Rb/^{86}Sr$ isochron plot for lava flows from Sjangeli and Unna Alakata (cf. Fig. 1). STD*x* samples are from different flows, D*x* samples are from a strongly fractionated flow or hypabyssal dike. Data from Table 2. B. Mixing diagram for the same data for 0 My and recalculated to 2250 My. C. Correlation of mixing line for different times of recalculation. Note the maximum near 2200 My for D*x* samples. The change of sign after 2300 My only indicates a negative slope of the mixing line. For discussion see text.

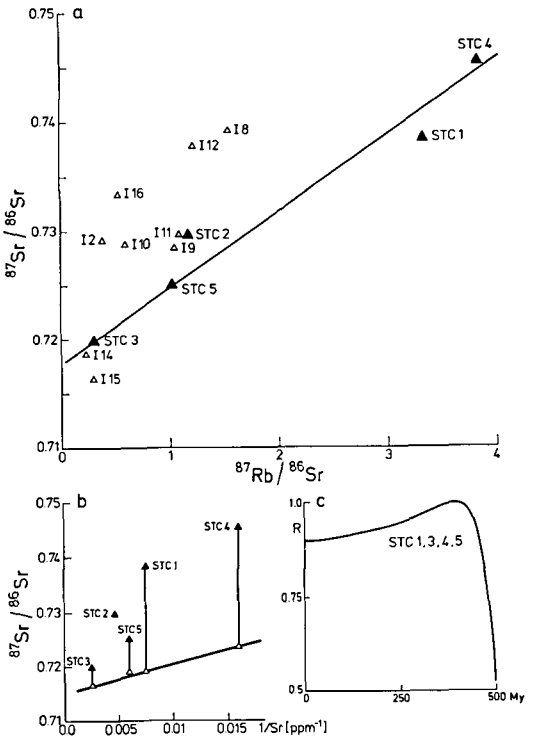

Fig. 5. A. $^{87}Sr/^{86}Sr$ - $^{87}Rb/^{86}Sr$ correlation diagram for tuffs from Sjangeli (cf. Fig. 1). STC*x* samples are from one layer, while I*x* samples represent a profile across the layering. Data from Table 2. B. Mixing diagram for the same data for 0 My and recalculated to 400 My. C. Correlation of mixing line for different times of recalculation. Note the maximum near 400 My. For discussion see text.

For the Rb-Sr system of the tuffs the mixing calculations yield a maximum fit of the mixing line at 400 My. Similarly, for the Pb-Pb system of the lava flows and the metamorphosed basic dike, the best fit of the anomalous lead line is obtained for 425-465 My and 430-470 My, respectively.

The occurrence of maxima in the mixing diagram for the Rb-Sr system of the STC*x* samples at c. 400 My and for the Pb-Pb system in the lava flows at c. 425-465 My strongly suggests open system behavior of these systems during the Caledonian orogeny with mixing of the Sr isotope composition and the Pb isotope composition. The difference of the mixing times for the Rb-Sr and the Pb-Pb system could be real, but could as well be an artifact from the recalculation procedure, since the propagation of analytical errors through the recalculation procedure could shift the maxima. For model calculations, the time of the Caledonian disturbance is arbitrarily set to 430 My.

Rb-Sr isotope data

All Rb-Sr isotope data have been tested for mixing using the above described principles. Isochron plots, mixing diagrams and time-regression variograms for the lava flows, and for the tuffs which enclose the lava flows, are shown in Figs. 4 and 5. Although both lithological units are Proterozoic, the lava flows have yielded an Early Proterozoic age while the tuffs give a Caledonian age.

Lava flows. Five whole-rock samples from lava flows and four whole-rock samples from a metamorphosed basic dike have been analyzed. (Because of the similar behavior of the Rb-Sr isotope system, the dike is discussed together with the metalava flows). The samples fall on two different trends with similar slopes, but with significantly different Sr-initials (cf. Fig. 4).

Three (STD4, STD6, STD7) of the five lava flow samples define a regression line which yields an age of 2324 ± 15 My (MWSD = 0.312). The isotope system of the remaining two samples is disturbed. Their Rb and Sr had been redistributed and homogenized over distances larger than the sample volume, which for the whole-rock samples was 3 to 5 dm^3.

Three (D1, D2, D5) of four samples from the dike also define a regression line, which gives a date of 2252 ± 71 My (MWSD = 21.15).

The isotopic composition of Sr from these two sets of samples has been recalculated for mixing plots. These mixing plots (Fig. 4, part B) indicate no mixing for the Rb-Sr whole-rock system of these samples during either the Caledonian or the Svecokarelian orogeny and metamorphism. However, it is possible that there had been mixing at about 2200 My (cf. Fig. 4, part C). The whole-rock samples show at that time the best fit to a straight line in the mixing plot (Fig. 4, part B). The line for both sets of samples is tilted, indicating that the two mixed components had isotopically different compositions and that therefore the 'isochron' probably yields an age too high by about 100 My to 150 My. If this mixing is real, it is probably related to the extrusion of the lava flows or the intrusion of the metamorphosed basic dikes. Possible sources of the contaminating Sr could be assimilated wall rock or sea-water.

The high value of the Sr-initial of the D*x* samples indicates that these rocks probably contain Sr which had evolved in a high Rb/Sr environment, such as continental crustal rocks. The high Sr-initial could be due to selective breakdown of high Rb/Sr phases, such as biotites, and does not reflect the bulk $^{87}Sr/^{86}Sr$ ratio of the contaminating crustal rocks. Quartzites and metaconglomerates in the Kopparåsen area indicate an older silicic crust in the vicinity of the Sjangeli area.

Mineral separates from three different lava flows have been analyzed (Table 2, Fig. 6). The Rb-Sr data of these mineral concentrates demonstrate that the Rb-Sr isotope system, on a mineral scale, had been disturbed.

(1) The analyzed mineral phases are metamorphic, and the Rb-Sr system for these phases and the whole-rock should yield the time of metamorphism. However, the mineral separates have isotopic compositions that do not align on a linear array. This implies that the mineral isotope system, if it ever fulfilled the conditions for an isochron, was disturbed by a later metamorphic event, which was insufficient to reset the Rb-Sr system completely.

(2) The isotopic composition of minerals with similar Rb/Sr ratios is different beyond analytical error for any time of recalculation (cf. epidotes of flow STD4). The Sr composition of e.g. epidote is a mixture of two isotopi-

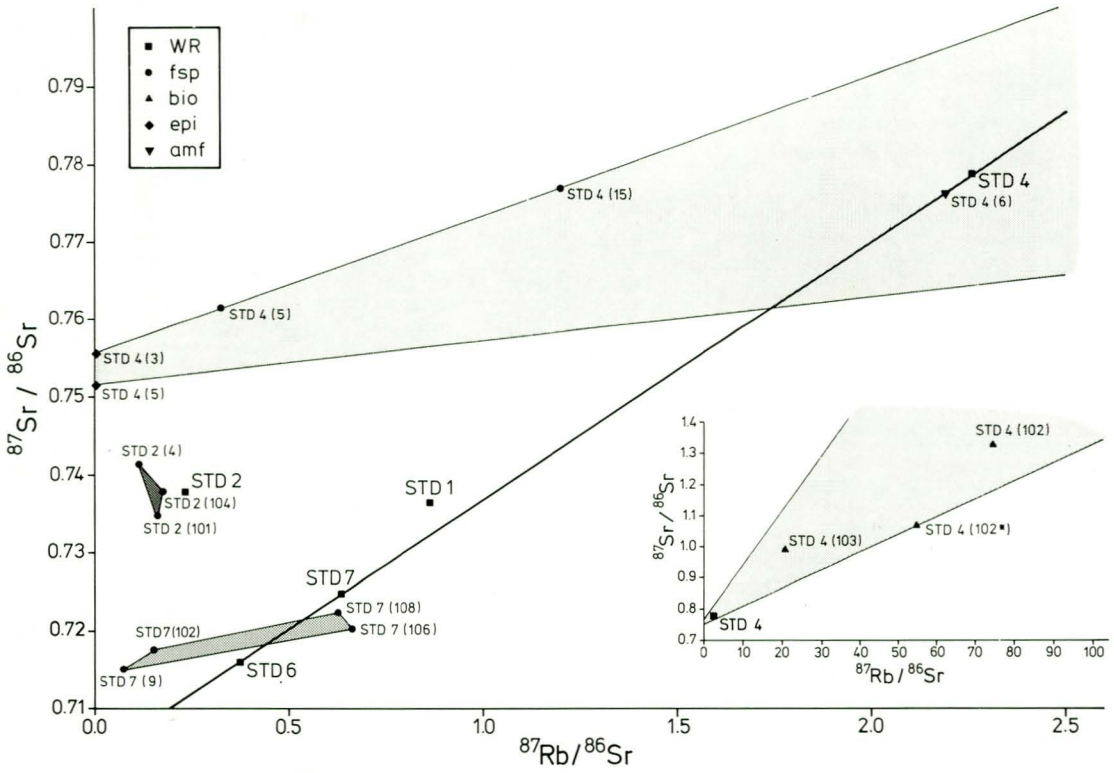

Fig. 6. $^{87}Sr/^{86}Sr$ - $^{87}Rb/^{86}Sr$ correlation diagram for basic lava flows from the Sjangeli area. STD*x* samples are whole-rock samples from different flows. Flow STD2 is strongly sheared and all measured isotope systems are disturbed. Numbers in parentheses refer to the original sample code (Romer 1987; Appendix V). Note that the whole-rock samples have a considerably better linear alignment than the mineral separates. The whole-rock line represents a reference date of 2324 My with an apparent initital of 0.7034. Shaded area (for STD2 and STD7) represents the field of minimum variation of the isotopic composition of feldspar, and for STD4 it represents the mixing field between the steepest and flattest envelope of STD4 mineral compositions. Insert shows STD4 minerals with high radiogenic Sr-compositions (note the scale difference).

cally different Sr components, and there had been non complete rehomogenization by diffusion.

(3) Since *all* mineral samples are in disequilibrium with the whole-rock sample, no ages can be calculated. However, the occurrence of metamorphic minerals with strongly disturbed isotopic interrelationships indicates that there had been at least two metamorphic phases, one for the formation of these minerals, and one for the disturbance of the isotopic systems of these minerals. Further, the two phases must have been separated from each other in time, in order to allow for the generation of sufficient radiogenic Sr to yield high $^{87}Sr/^{86}Sr$ ratios. Assuming that the biotites were in equilibrium with a common Sr with a geologically reasonable composition ($^{87}Sr/^{86}Sr$ = 0.7515 i.e. epiodote), the model dates foı biotites indicate values between 405 My and 730 My.

A possible interpretation of these variable model ages is that they result from mixtures of two differently 'aged' biotite generations. The younger model age could derive from biotite which was isotopically completely reset during the Caledonian orogeny or which formed at that time. The older model ages represent mixtures with variable ratios of older to younger biotite, whereby the older biotite also has lost Rb and Sr to a variable extent during the formation of the younger biotites. The older component is possibly of midproterozoic age as suggested from Pb-Pb and Sm-Nd data (see below). If the younger model age also represents a mixture, then the younger biotite has to be younger than c. 405 My. A

lower intital Sr composition ($^{87}Sr/^{86}Sr$ = 0.704) would increase the biotite model ages to values between 465 My and 890 My; however, the qualitative interpretation is not changed. The presence of two, in time widely separated, greenschist-facies metamorphisms is also indicated by the lead isotope data.

Tuffs. Tuffs from Sjangeli (Fig. 1) have been sampled along two profiles, one parallel to (STC*x*) and the other across the strike (I*x*) of the volcanites. The STC*x* samples have been taken within the same tuff layer over a distance of 50 m. They define a 'scattery' regression line with an apparent age of 488 ± 64 My. However, mixing plots demonstrate that the samples fit the conditions for mixing, and that the best fit of the mixing line is obtained for 400 My. The good fit of the mixing line to the STC*x* samples strongly contrasts with the poor fit of the I*x* samples to any linear trend in an isochron diagram (Fig. 5) or a mixing diagram.

If there is a higher permeability parallel to, rather than across the schistosity (cf. Etheridge et al. 1983), then the fluids migrate within the same layer. If these fluids were in equilibrium only with the layer in which they flowed, then the isotopic composition of the fluids in the various layers would have varied. The poorer fit of the mixing line and the lack of an isochron to the I*x* samples may relect different isotopic characteristics in the various layers. Further, the isotopic exchange may have been less across the layers, than within the layers.

Mineral isotope data from STC1 and STC4 show the same disequilibrium relationships as the mineral samples from the lava flows. Note that the isotopic homogenization and mixing was more complete between the various STC*x* whole-rock samples, than between the different mineral phases in a single whole-rock sample.

Sm-Nd isotope data

In the $^{143}Nd/^{144}Nd$ - $^{147}Sm/^{144}Nd$ correlation diagram, mineral separates from most units plot in a field instead of along a line. This is examplified by the Sm-Nd isotope data from minerals from lava flow STD4 and amphibolite STA1 (Fig. 7, Table 3). However, the STA1 mineral separates define a linear field, which

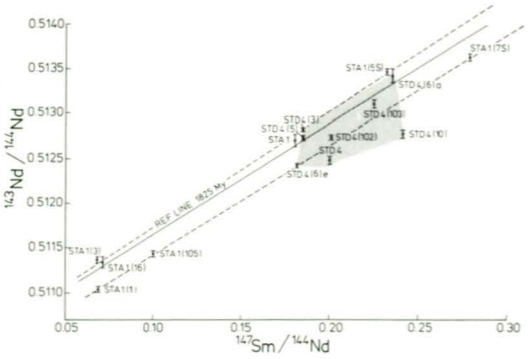

Fig. 7. $^{143}Nd/^{144}Nd$ - $^{147}Sm/^{144}Nd$ correlation diagram for mineral separates from amphibolite STA1 and metalava flow STD4. Note that none of the mineral whole-rock systems forms an isochron. Reference line by equally weighing all samples. Dashed lines represent envelopes through most radiogenic and least radiogenic STA 1 mineral separates, respectively.

yields a reference date of 1825 ± 173 My if all samples are weighed equally. Although no age is deducible from the STA1 mineral separates, which are in isotopic disequilibrium with each other due to (1) later disturbance or (2) incomplete isotopic homogenization at the time the system formed, the STA1 isotope data clearly demonstrate that the system is Proterozoic. Since the STA1 isotope system is bound to amphibolite-facies minerals, this strongly indicates that the amphibolite-facies metamorphism was Proterozoic although the exact age is not known. Possibly this metamorphism is related to the intrusion of the midproterozoic granites and syenites.

Pb-Pb isotope data

Lava flows. The lead isotopic composition of the lava flow whole-rock samples has been recalculated for different times. The recalculation results in a better fit of the whole-rock samples to a straight line, except for sample STD6 in the $^{206}Pb/^{204}Pb$ - $^{207}Pb/^{204}Pb$ diagram (Fig. 8). The best fit for the whole-rock samples is obtained for c. 425-465 My, while recalculation times larger than c. 500 My decrease the alignment along a straight line. This strongly suggests that there had been a disturbance of the whole-rock lead system of the lavas at c. 425-465 My. The whole-rock lead composition (recalculated to 430 My) is shown in Fig. 9.

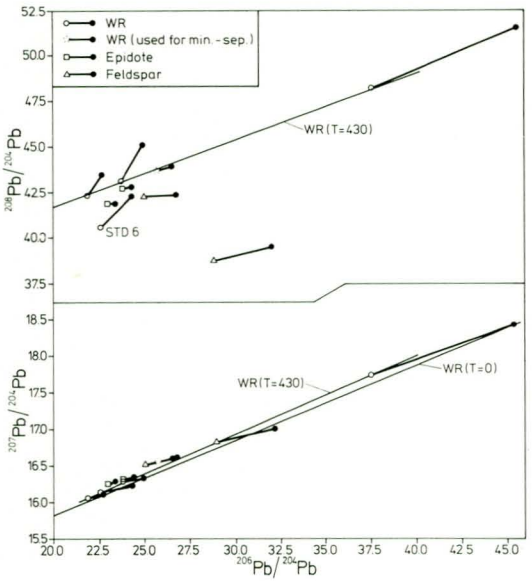

Fig. 8. $^{206}Pb/^{204}Pb$ - $^{207}Pb/^{204}Pb$ and $^{206}Pb/^{204}Pb$ - $^{208}Pb/^{204}Pb$ correlation diagram for lava flows from the Sjangeli area. The values are shown for present day (full symbols) and recalculated for 430 My (open symbols). Note the different isotopic compositions of minerals (STD4) and whole-rock at 430 My. The compositional variation in the $^{206}Pb/^{204}Pb$ - $^{208}Pb/^{204}Pb$ diagram cannot be explained by a simple two component mixing at 430 My. An additional phase with thorogenic lead is necessary to explain the position of the feldspar trace lead composition.

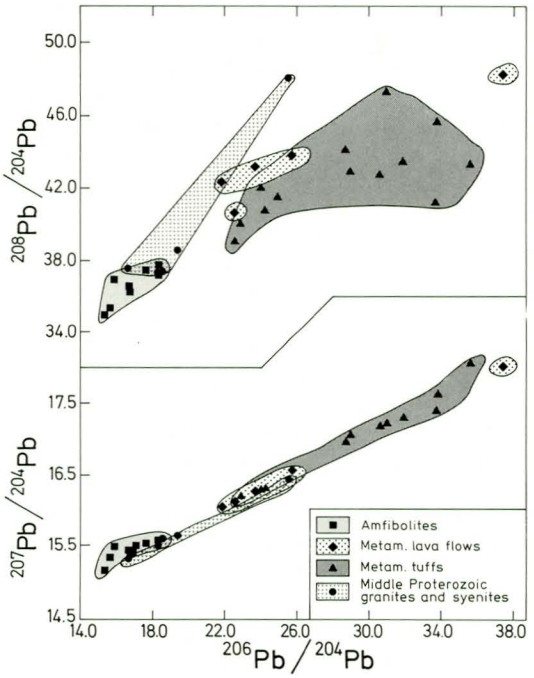

Fig. 9. Whole-rock lead composition, recalculated to 430 My, from the various units of the Sjangeli area.

If this Caledonian disturbance had resulted in a complete rehomogenization of the isotopic composition, then the recalculated lead composition of all mineral phases should coincide with their whole-rock composition. This is not the case (Fig. 8) and, therefore, the variation of the lead composition of epidote and plagioclase cannot be explained by *in-situ* formed radiogenic lead alone.

The spread of the $^{206}Pb/^{204}Pb$ - $^{207}Pb/^{204}Pb$ ratio indicates mixing of at least two different lead components. Mixing is also indicated by the negative correlation of the contents of ^{204}Pb lead and the radiogeneity of lead, recalculated to 430 My. The samples with a lower ^{204}Pb lead content would have a higher degree of contamination by radiogenic, externally derived lead.

An interpretation of the whole-rock lead line as a mixing line of cogenetic mixing components, using 430 My as the time of mixing, would yield a model age of 1810 ± 20 My.

While such a simple mixing model can explain the variation of the $^{206}Pb/^{204}Pb$ - $^{207}Pb/^{204}Pb$ ratios, it is insufficient to explain the $^{206}Pb/^{204}Pb$ - $^{208}Pb/^{204}Pb$ variations. The thorogenic lead indicates that (at 430 My) there were at least three different lead components present. The three components were (1) the primary lead from the time of the crystallization of epidote and plagioclase; (2) the radiogenic lead from *in-situ* decay of U and Th from that time to the time of disturbance; and (3) an externally derived contaminating component. If the components (2) and (3) had evolved in environments characterized by different κ ($^{232}Th/^{238}U$) ratios, then a mixture of these two and component (1) will not form a linear trend (Fig. 8). From the $^{206}Pb/^{204}Pb$ - $^{208}Pb/^{204}Pb$ lead diagram (Fig. 8) it is obvious that the plagioclase lead must have evolved in an environment with a lower κ ratio than the whole-rock samples or the epidotes. If feldspar has a lower κ ratio than its whole-rock sample (as suggested by

data from Gray & Oversby 1972, Tilton et al. 1955), the low-thorogenic component could represent an old feldspar lead, i.e. the feldspars are, at least partially, much older than the Caledonian mixing event. If the low-thorogenic lead component of the feldspars is, alternatively, attributed to the addition from an externally derived fluid, then the feldspar lead should plot on the same lead line as the whole-rock samples which obtained an external lead contribution. Since the feldspar lead plots below the whole-rock lead line in the $^{206}Pb/^{204}Pb$ - $^{208}Pb/^{204}Pb$ diagram, the presence of an old feldspar component is possible.

The mineral separates are greenschist-facies minerals. Since there are at least three different lead components present, the lead composition of these greenschist-facies minerals cannot be explained by a formation during the Caledonian orogeny with the addition of an external lead component. The greenschist-facies minerals have to originate from an earlier metamorphism, and have later, during the Caledonian orogeny, acquired an additional lead component.

The lead composition of the four D*x* samples is higly radiogenic (Table 4). In an $^{206}Pb/^{204}Pb$ - $^{207}Pb/^{204}Pb$ lead correlation diagram, these samples fit a lead line yielding an age of 2083 ± 20 My. A recalculation of the lead composition similar to the method used for the lava flows (Welke & Nicolaysen 1981) changes the lead line age only slightly (2093 ± 25 My, for a recalculation to 400 My), but leads for times greater than 470 My strongly increase the scatter around the lead line.

All four samples have high contents of thorogenic lead, and they do not form a linear array in the $^{206}Pb/^{204}Pb$ - $^{208}Pb/^{204}Pb$ correlation diagram. However, the recalculation of the lead composition improves the fit of the regression line in the $^{206}Pb/^{204}Pb$ - $^{208}Pb/^{204}Pb$ diagram, indicating a disturbance of the U-Th-Pb system at about 430—470 My, where the best fit of the regression line is obtained. Note that the best-fit times for the $^{206}Pb/^{204}Pb$ - $^{207}Pb/^{204}Pb$ (c. 430 My) and $^{206}Pb/^{204}Pb$ - $^{208}Pb/^{204}Pb$ (c. 470 My) systems do not coincide. The model age variation, with the recalculation, demonstrates the polystage nature of the lead line.

Tuffs. The tuffs have a more radiogenic lead composition than the lavas (Fig. 9). The recalculation of the lead composition of the tuffs results in an age variation (similar as for the lavas) and therefore indicates a multistage lead growth. The beginning of the last stage is set to 430 My in concordance with the model ages used for, e.g., the lava flows (see section on the mixing lines).

At about 430 My the ω ($^{232}Th/^{204}Pb$) ratio of, e.g., samples I8 and I9 was significantly altered. These two samples had high Th concentrations and high ω ratios. However, they could not have had high ω ratios for more than the last c. 430 My, since their high $^{208}Pb/^{204}Pb$ ratio is compensated at c. 430 My. They must have had a lower ω ratio prior to c. 430 My. The increased ω ratio could be due to an addition of Th, loss of Pb, or both.

Other samples, e.g. I10, indicate that there must also have been a change of the μ ($^{238}U/^{204}Pb$) ratio at c. 430 My, since the excess radiogenic lead of this sample is compensated for at c. 430 My.

The change of the ratios between U, Th, and Pb at c. 430 My indicates that the rocks behaved as open systems and were sufficiently permeable to allow for the efficient transport of at least two of these three elements.

The radiogenic composition of the trace lead of the tuff could be explained by the infiltration of a radiogenic lead component or by an earlier enrichment of U. Romer (1989) has demonstrated with data from sulfide mineralizations from the Sjangeli area, which occur in the tuffs and quartz-mica schists, that there had been at least two events of U/Th separation and of changes of the μ ratios. One of these events was an U-infiltration at c. 400—500 My, while the other event was an U-infiltration at c. 1600—1800 My. Such a Proterozoic U-enrichment could explain the scatter of the tuff trace lead composition in the $^{206}Pb/^{204}Pb$ - $^{207}Pb/^{204}Pb$ lead diagram.

Amphibolites. The amphibolites have the least radiogenic whole-rock lead composition of the analyzed samples from the Sjangeli area (Fig. 9). There had been an addition of radiogenic lead to the trace lead of the sulfide mineralizations, within the tuffs at Unna Alakats and Sjangeli (cf. Fig. 1). Model calculations have shown that this lead addition occurred at c. 430 My (cf. Romer 1989). The lead could have been derived from the wallrock or from an external reservoir. However, independent of the source, the tuffs had to be permeable enough to allow the migration of Pb into the sulfide mineralizations. In contrast, most amphibolites did not obtain such an external lead component.

Some amphibolites (STA4, A22, A29) have μ ratios which indicate a U-enrichment at about 400 My to 500 My ago. This suggests that at least some of the amphibolites had been subjected to element redistributions, for example through infiltration of uranium.

Acid intrusions. The granites and syenites have a lead composition (Fig. 9) which had evolved in a higher κ ($^{232}Th/^{238}U$) environment than that of the other rocks from the Sjangeli area (with the exception of the metamorphosed basic dikes).

The different composition of the lead of the intrusive rocks, in comparison to the tuffs, eliminates the granites as the source for the radiogenic lead which had infiltrated the tuffs. Little or no lead transport occurred between these two units. This implies that the granites/syenites had a small range of Pb mobility, in contrast to the tuffs.

Time constraints from the isotope data

The lead isotopic composition of the whole-rock samples of the basic volcanites apparently correlates with the extent of retrogression of the metamorphic mineral assemblage. The least retrogressed rocks, the amphibolites, have the least radiogenic lead, while the most retrogressed, the tuffs, show the highest radiogenic lead composition and the largest variation of lead radiogeneity (Fig. 9). This relationship suggests that the retrogression was accompanied by the addition of radiogenic lead, U, and/or Th into the basic volcanites. The time of disturbance of the lead system can therefore be used to estimate the time of retrogression.

The best fit of the mixing lines for c. 400 My (cf. Fig. 5 part C) indicates that during the Caledonian orogeny the whole-rock Rb-Sr system of the tuffs had been open. Sr must have migrated over distances larger than the sample volume in order to cause isotopic mixing (Roddick & Compston 1977). This implies that the tuffs had been permeable, and that there must have been a fluid present to allow the effective migration of Sr.

The isotopic mixing of the tuffs and lavas during the Caledonian orogeny did not result in an isotopic homogenization of the mineral isotope systems. The Rb-Sr compositions of biotite, albite and epidote indicate that these minerals have experienced more than one evolution stage. They all can be modelled as two component mixtures of an old component (Proterozoic) and a young component (Caledonian) which have mixed in varying ratios. This would imply that there had been an older pre-Caledonian crystallization of albite, biotite, and epidote. During the Caledonian metamorphism there would have been an additional growth of these phases and a partial opening of the pre-Caledonian minerals by recrystallization or, in the base of biotite, by chloritization.

The mechanical separation of mineral phases of these two different generations was not possible, since they have very similar or identical physical properties. The measured isotopic ratios of minerals therefore represent mixtures, in varying portions, of the different generations of the same mineral. This polyphase character of the various minerals is most obvious in the Rb-Sr and the $^{206}Pb/^{204}Pb$ - $^{208}Pb/^{204}Pb$ correlation diagrams for the lava flows (Figs. 6 and 8, respectively).

The presence of a pre-Caledonian metamorphism is further indicated by the Sm-Nd data from the amphibolite STA1. The analyzed mineral separates yield a reference line indicating a date of 1825 ± 173 My. The large scatter about the reference line indicates that the mineral system had been disturbed by a later event, which however did not result in a homogenization of the system.

The isotope data do not give isochrons for the metamorphic events, and therefore they do not give exact ages for the two metamorphisms. However, they clearly indicate that there had been partial isotopic resetting during the Caledonian metamorphism, and that there had been a Middle Proterozoic metamorphism. Further, the greenschist-facies mineral assemblages of the lavas and tuffs have isotopic compositions which strongly suggests that part of these assemblages had been formed during the Proterozoic metamorphism.

The model

The Lower Proterozoic supracrustal rocks of the Sjangeli area have been metamorphosed at least twice. The first metamorphism recognized is a Svecokarelian regional metamorphism which reached amphibolite-facies conditions. The hornblende plagioclase geothermo-

barometer of Plyusnina (1982) yields maximum conditions of c. 6 kbar and c. 650°C. This metamorphism is of Lower to Middle Proterozoic age, as is suggested from the Sm-Nd mineral (fsp + bio + amf) reference line (1825 ± 173 My) using the amphibolite-facies minerals from the amphibolite, and from the lead model age of the lava flows (1810 ± 20 My). Regional Svecokarelian metamorphism (c. 1700 My) of higher grade (granulite and amphibolite facies), has, however, been described from the Vesterålen area (to the northwest of the Sjangeli area) by Griffin et al. (1978).

During the Svecokarelian orogeny and the coeval regional metamorphism, granites and syenites intruded the supracrustal rocks of the Sjangeli area. Rb-Sr dates for these intrusions indicate ages of 1780 ± 85 My (Gunner 1981) and 1691 ± 90 My (Heier & Compston 1969). The intrusions predated the mylonitization of the supracrustal rocks. The mylonites were located preferentially near the contacts between rigid units and less competent rocks (cf. Hobbs et al. 1976, p. 260).

The mylonitization occurred under lower grade conditions than the amphibolite-facies metamorphism and was associated with the infiltration of a fluid. The resulting retrogression of the amphibolite facies mineral assemblage to a greenschist-facies assemblage occurred at c. 4 kbar and c. 480°C.

These N-S striking mylonites are Svecokarelian structures, as is indicated by lead isotope data from the sulfide mineralizations in the mylonitized tuffs (Romer 1989). These data demonstrate that there had been a pronounced U-enrichment in some of the sulfide mineralizations and their wallrocks about 1600 My to 1800 My ago. Further, there are mineral isotope data from the lava flows and tuffs which indicate a possible Proterozoic age for the formation of the greenschist-facies mineral assemblage (cf. sections on isotope data).

The second metamorphism of the Sjangeli area is of Caledonian age. This metamorphism resulted in an overgrowth and partial recrystallization of the Proterozoic greenschist-facies mineral assemblage. Since most greenschist-facies minerals consist of several generations, at least one of which was Proterozoic, the isotopic systems represent mixtures and do not yield ages. The Rb-Sr whole-rock system of the tuffs shows a best fit to a mixing line at c. 400 My (Fig. 5), while the Pb-Pb whole-rock system of the lavas and the metamorphosed basic dike indicate mixing ages of ca. 425—470 My. If the difference is real, this could tentatively indicate that the change of the μ ratio was not necessarily related to the circulation of a metamorphic fluid. Instead, it may have been the result of the circulation of oxidized near-surface fluids, which circulated prior to the arrival of the Caledonian nappes, while the Rb-Sr system became mixed during the Caledonian metamorphism.

The Caledonian metamorphism resulted in the recrystallization of the greenschist-facies mineral assemblages. The distribution of the greenschist-facies mineral assemblage was confined to the same areas, which also showed the Proterozoic retrogression from the amphibolite facies. The observed greenschist-facies mineral assemblage therefore contains minerals from two different metamorphic events.

Locally the greenschist-facies rocks have been mechanically reactivated along steep shear zones and listric faults with vertical offsets up to some 100 m. This basement imbrication occurred subsequent to the thrusting of the Caledonian nappes and is largely a remobilization of old basement mylonite zones (cf. Bax 1989). The mixing of the Rb-Sr whole-rock isotope system of the tuffs, which is related to the basement reactivation, was associated with the fluid flow through the tuffs.

Conclusions

The basic volcanic units of the Sjangeli greenstone belt show greenschist-facies mineral assemblages along the borders of the belt and amphibolite facies in the central parts of the belt. The amphibolites give a P-T estimation of c. 6 kbar and c. 560°C. The other units (lava flows, pillow lavas, and tuffs) probably reached the same grade, however, they have been retrogressed to a greenschist-facies mineral assemblage. The retrogression is lithologically confined to the more deformed, schistose and/or mylonitized units.

The Rb-Sr whole-rock system of the basic lava flows at Sjangeli and the metamorphosed basic dike at Unna Alakats give dates of 2324 ± 15 My and 2252 ± 71 My, respectively. However, they probably represent mixing lines instead of isochrons and yield ages which are too high by c. 100 to 150 My (cf. Fig 4). The amphibolites yield a Sm-Nd data of 1825 ±

173 My for minerals, indicating a Proterozoic amphibolite-facies metamorphism. Since the greenschist-facies mineral assemblage formed during two different events, and did not become completely reset during the later, Caledonian metamorphism, they do not yield ages. However, the Pb-Pb isotope data from the lavas give lead lines which represent mixing lines of a Caledonian lead component (430 My) and a Proterozoic lead component (1810 ± 20 My).

The prograde amphibolite-facies metamorphism resulted in a homogenization of the isotopic initial composition between the different mineral phases, while the retrogression to greenschist facies was selective and did not result in a homogenization (Fig. 7). The whole-rock isotope system of the undeformed basic units was closed during the metamorphism, while the whole-rock isotope systems of the highly strained, schistose units, e.g. the tuffs and the lava flow STD2, were open, and mixed with the adjacent rocks.

Acknowledgements
I thank LKAB Prospektering Kiruna for support during the field seasons 1983 and 1984. I am grateful to G.R. Tilton for providing laboratory space at the University of California at Santa Barbara. An earlier draft of the manuscript benefited from critical comments by E. Sawyer, P.-G. Andreasson and an anonymous reviewer. I am grateful to Milan Vnuk (LuH) for skilfully drafting the figures and to Theresa M. Boundy for patiently correcting the language.

References

Barnes, S.-J., Boyd, R., Korneliussen, A., Nilsson, L.-P., Often, M., Pederson, R.B. & Robins, B. 1988: The use of mantle normalization and metal ratios in discriminating between the effects of partial melting, crystal fractionation and sulphide segregation on the platinum group elements, gold, nickel and copper: Examples from Norway. *In* Pritchard, H.M., Potts, P.J., Bowles, J.F.M. & Cribb, S.J. (eds.), *Geoplatinum 87, conferrence volume.* Elsevier Amsterdam, 113–143.

Bax, G. 1986: Basement involved Caledonian nappe tectonics in the Swedish part of the Rombak-Sjangeli window. *Geol. Fören. Förh. 108,* 268–270.

Bax, G. 1989: Caledonian structural evolution and tectonostratigraphy in the Rombak-Sjangeli window and its covering sequences, Northern Scandinavian Caledonides. *Nor. geol. unders. Bull.* (this volume).

Beach, A. 1976: The interrelations of fluid transport, deformation, geochemistry and heat flow in early Proterozoic shear zones in the Lewisian complex. *Phil. Trans. R. Soc. London A 280,* 569–604.

Bergström, J. & Gee, D.G. 1985: The Cambrian in Scandinavia. *In* D.G. Gee & B.A. Sturt (eds.) *The Caledonian orogen – Scandinavia and related areas.* John Wiley & Sons Ltd., Chichester, 247–271.

Bird, D.K. & Helgeson, H.C. 1981: Chemical interaction of aqueous solutions with epidote-feldspar mineral assemblages in geologic mineral assemblages in geologic systems. *II Equilibrium constraints in metamorphic/ geothermal processes. Am. J. Sci. 281,* 576–614.

Bryhni, I. & Andreasson, P.-G. 1985: Metamorphism in the Scandinavia Caledonides. *In* D.G. Gee & B.A. Sturt (eds.) *The Caledonian orogen - Scandinvian and related areas.* John Wiley & Sons Ltd., Chichester, 763–781.

Cameron, A.E., Smith, D.H. & Walker, R.L. 1969: Mass spectrometry of nanogram-size samples of lead. *Analyt. Chem. 41,* 525–526.

Etheridge, M.A., V.J. Wall & Vernon, R.H. 1983: The role of the fluid phase during regional metamorphism and deformation. *J. metamorphic Geol. 1,* 205–226.

Faure, G. 1986 (2nd ed.): *Principles of isotope geology.* Wiley & Sons, New York, 589 pp.

Gaal, G. & Gorbatschev, R. 1987: An outline of the Precambrian evolution of the Baltic Shield. *Prec. Res. 35,* 15–52.

Geijer, P. 1924: Some Swedish occurrences of bornite and chalcocite. *Sver. geol. unders. Ser. C 321,* 52pp.

Gray, C.M. Oversby, V.M. 1972: The behaviour of lead isotopes during granulite facies metamorphism. *Geochim. Cosmochim. Acta 36,* 939–952.

Griffin, W.L., Taylor. P.N., Hakkinen, J.W., Heer, K.S., Iden, I.K., Krogh, E.J., Malm, O., Olsen, K.I., Ormaasen, D.E. & Tveten, E. 1978: Archean and Proterozoic crustal evolution in Lofoten-Vesterålen, N Norway. *J. geol. Soc. London 135,* 629–647.

Grip, E. & Frietsch, R. 1973: *Malm i Sverige II.* Amsell & Wiksel, Uppsala, 295 pp.

Grünenfelder, M., Tilton, G.R., Bell, K. & Blenkinsop, J. 1986: Lead and strontium isotope relationships in the Oka carbonatite complex, Quebec. *Geochim. Cosmochim. Acta 50,* 461–468.

Gunner, J.D. 1981: A reconnaisance Rb-Sr study of Precambrian rocks from the Sjangeli-Rombak window and the pattern on initial $^{87}Sr/^{86}Sr$ ratios from Northern Scandinavia. *Nor. Geol. Tidsskr. 61,* 281–290.

Heier, K.S. & Compston, W. 1969: Interpretation of Rb-Sr age patterns in high grade metamorphic rocks, North Norway. *Nor. Geol. Tidsskr. 459,* 257–283.

Hickman, M.H. & Glassley, W.E. 1984: The role of metamorphic fluid transport in the Rb-Sr isotopic resetting of shear zones: evidence from Nordre Strømfjord, West Greenland. *Contrib. Mineral. Petrol. 87*, 265–281.

Hobbs, B.E., Means, W.D. & Williams, P.F. 1976: *An outline of structural geology*. 571 pp., Wiley & Sons, New York.

Jensen, L.S. 1976: A new cation plot for classifying subalkalic volcanic rocks. *Ontario Div. Mines miscel. Pap. 66*, 22pp.

Korneliussen, A., Tollefsrud, J.I., Flood, B. & Sawyer, E. 1986: Precambrian volcano-sedimentary sequences and related ore deposits, with special referance to the Gautelisfjell carbonate-hosted, disseminated gold deposit, Rombaken basement window, Northern Norway. *Nor. geol. unders. Unpubl. report 86.193*, 43pp.

Kulling, O. 1964: Översikt över norra Norrbottensfjällens Kaledonberggrund, Karta Skala 1:400 000. *Sver. geol. unders. Ba 19*, 166pp.

Laird, J. & Albee, A.L. 1981: High-pressure metamorphism in mafic schists from northern Vermont. *Am. J. Sci. 281*, 97–126.

Leake, B.E. 1978: Nomenclature of amphiboles. *Canadian Mineral. 16*, 501–520.

Lindqvist, J.-E. 1987: Metamorphism in basement rocks and the implication for the tectonic evolution, Nasafjäll Window, Scandinavian Caledonides. *Geol. Rundsch. 76*, 837–850.

Moody, J.B., Meyer, D. & Jenkins, J.E. 1983: Experimental characterization of the greenschist/amphibolite boundary in mafic systems. *Am. J. Sci. 283*, 48–92.

Petersson, W. 1897: De geologiska förhållandena i trakten omkring Sjangeli Kopparmalmsfält i Norrbottens län. *Sver. geol. unders. Ser. C 171*, 13pp.

Plyusnina, L.P. 1982: Geothermometry and geobarometry of plagioclase-hornblende bearing assemblages. *Contrib. Mineral., Petrol. 80*, 140–146.

Richard, P., Shimizu, N. & Allégre, C.J. 1976: $^{143}Nd/^{144}Nd$, a natural tracer: An application to oceanic basalts. *Earth Planet. Sci. Lett. 31*, 269–278.

Robinson, P., Spear, F.S., Schumacher, J.C., Leirad, J., Klein, C., Evans, B.W. & Doolan, B.L. 1982: Phase relations of metamorphic amphiboles: Natural occurrence and theory. *In* D.R. Veblen & P.H. Ribbe (eds.) *Amphiboles: Petrology and experimental phase relations*. Mineral. Soc. Am. Rev. in Mineral. 9B, 1–227.

Roddick, J.C. & Compston, W. 1977: Strontium isotope equilibration: A solution to a paradox. *Earth Planet. Sci. Lett. 34*, 238–246.

Romer, R.L. 1987: The geology, geochemistry and metamorphism of the Sjangeli area, a tectonic window in the Caledonides of Northern Sweden. *Research report, Luleå University, Sweden.* TULEA 1987:16, 124pp.

Romer, R.L. 1989: Interpretation of the lead isotopic composition from sulfide mineralizations in the Proterozoic Sjangeli area, Northern Sweden. *Nor. geol. unders. Bull.* (this volume).

Sawyer, E. 1986: Metamorphic assemblages and conditions in the Rombak basement window. *Nor. geol. unders. Unpubl. report* 86.168.

Skiöld, T. 1986: On the age of the Kiruna greenstones, Northern Sweden. *Prec. Res. 32*, 35–44.

Skiöld, T. 1987: Aspects of the Proterozoic geochronology of northern Sweden. *Prec. Res. 345*, 161–167.

Spear, F.S. 1982: Phase equilibria of amphibolites from the Post pond volcanics, Mt Cube Quadrangle, Vermont. *J. Petrol. 23*, 383–426.

Steiger, R.H. & Jäger, E. 1977: Subcommission on geochronology: Convention on the use of decay constants in geo- and cosmochronology. *Earth Planet. Sci. Lett. 36*, 359–362.

Tilton, G.R., Patterson, C., Brown, H., Inghram, M., Hayden, R., Hess, D. & Larsen, E. jr. 1955: Isotopic composition and distribution of lead, uranium, and thorium in a Precambrian granite. *Bull. Geol. Soc. Am. 66*, 1131–1148.

Todt, W., Cliff, R.A., Hanser, A. & Hoffmann, A.W. 1984: $^{202}Pb + ^{205}Pb$ double spike for lead isotopic analyses. *Terra Cognita 4*, p. 209.

Tull, J.F., Bartley, J.M., Hodges, K.V., Andresen, A., Steltenpohl, M.G. & White, J.M. 1985: The Caledonides in the Ofoten region (68° - 69° N), north Norway: key aspects of tectonic evolution. *In* D.G. Gee and B.A. Sturt (eds.) *The Caledonian orogen — Scandinavia and related areas*. John Wiley & Sons Ltd., Chichester, 553–568.

Vollmer, R. 1976: Rb-Sr and U-Th-Pb systematics of alkaline rocks: the alkaline rocks from Italy. *Geochim. Cosmochim. Acta 40*, 283–295.

Wasserburg, G.J., Jacobsen, S.B., DePaolo, D.J., McCulloch, M.T. & Wen, T. 1981: Precise determination of Sm/Nd ratios, Sm and Nd isotopic abundances in standard solutions. *Geochim. Cosmochim. Acta 45*, 2311–2323.

Welke, H. & Nicolaysen, L.O. 1981: A new interpretative procedure for whole rock U-Pb systems applied to the Vredefort crustal profile. *J. Geoph. Res. 86*, 10681–10687.

White, W.M. & Patchett, J. 1984: Hf-Nd-Sr isotopes and incompatible element abundances in island arcs: implications for magma origins and crust-mantle evolution. *Earth Planet. Sci. Lett. 67*, 167–185.